ASCE 2020 Symposium 2 Exploration and Utilization of Extra-Terrestrial Bodies

Robotic Mobility in Extreme Terrain

Lunar Rover Optimization Platform for Wheel Traction Studies

Stephen Gerdts[1], John Breckenridge[1], Kyle Johnson[1]

[1]*NASA Glenn Research Center, Materials and Structures Division, Cleveland, OH 44135*

Abstract

Robotic mobility systems expand the reach of future scientific and exploration missions to celestial bodies. Understanding the traction performance of these systems is necessary knowledge that informs mission-level requirements, such as power budgets and navigation envelopes. This paper covers the design, development, and verification of the four wheeled Lunar Rover Optimization Platform (LROP). This mass optimized platform is targeted to emulate future medium class rovers weighing up to 90 kg. The LROP has the ability to conduct various wheel design experiments such as obstacle traversal, slope ascent, and drawbar pull over a wheel loading range of 4.5 to 22.7 kg. The platform also has the ability to shift its center of gravity (CG) laterally and longitudinally to explore the CG shift effects on mobility performance. This knowledge is valuable for future rover designers exploring different payload packaging solutions. In this paper results from obstacle traversal test with varying angle of attack (AOA) and longitudinal CG position are reported along with results from slope ascent testing which proved-out the LROPs capabilities.

1. Introduction

A rising interest for exploration of celestial bodies has reinvigorated research into surface science and In-Situ Resource Utilization (ISRU). Mobility systems become necessary facilitators for these endeavors as they act as a work multiplier. A roving science platform, like the Martian Research Laboratory (MRL), can visit multiple target geological sites as it investigates the rock record of other worlds. This is far more efficient than using multiple landers. The rock record can help us understand the climate histories of these worlds and can tell us what resources we can count on for ISRU. Resources such as water ice and metallic oxides create another mission for mobility platforms as their excavation and transportation becomes key for sustainable missions like a continuous human habitation. These missions create the need of another type of rover, a work rover. Not meant to carry scientific instrumentation, a work rover exist to undertake repetitive tasks too time or energy intensive for humans. The lunar roving vehicle (LRV) is an example of a work rover whose primary mission was to ferry astronauts. However, the LRV was a large class rover with a dry mass of 218 kg and gross mass of 708 kg, empty plus payload (Costes 1972). It also required direct user input during operation and was only designed to last 3 days.

With the increasing push for a sustainable human presence on the lunar surface there will be a need for medium class autonomous or remote controlled rovers. Medium class rovers such as the Martian Exploration Rovers (MER) Spirit and Opportunity have been flight proven. Their architectures were optimized for their missions and because of this they were able to log 52 km travel. To achieve this success NASA and JPL developed a series of analogue rovers to prove-out mobility, communications, and navigation. Rovers such as FIDO, rocky7, rocky8, and K9 served as central integration platforms and helped ground teams understand the performance of their mobility system (Tunstel 2002). These rovers took time to design and build as the parametric nature of spaceflight usually does. Future rover developers might not have the resources that NASA has to be able to develop and test multiple analogue rovers.

A recent push for future medium class rover development has been sparked by future lander contracts under the Commercial Lunar Payload Services (CLPS) program. Companies making landers for this program will be able to deliver up to 100 kg of payload to the surface of the moon. This opens the door to the moon for many organizations wishing to deliver small to medium class rovers. A need to be able to quickly test mobility variables like wheel dimensions and center of gravity (CG) for these future rovers is the motivation for this paper and for the Lunar Rover Optimization Platform (LROP). The mobility configurations will need to be proved out before launch and preferably during preliminary design. The LROP was designed to aid in the validation of requirements for future rovers such as slope ascent angle, obstacle height traversal, and wheel slip. The LROP has the ability to change its CG, accommodate wheels up to 65 cm in diameter, and generate wheel loads of up to 22.7 kg. This paper will discuss the design of the LROP as well as report the results from preliminary checkout testing that was conducted.

2. LROP Design

2.1 Frame

The critical design parameter of the platform was weight. The lighter the platform the more payload it could accommodate meaning a larger range of wheel loads. Knowing the CLPS landers could accommodate 90 kg payloads it was desirable to create a platform that could represent a four wheeled rover of that mass to anticipate the need of characterizing mobility solutions of that class. In order to size the platform a target dry weight (platform with no added payload) of 20 kg was selected, leaving up to 70 kg available for payload in order to obtain a wheel loading range of 5 - 22.5 kg.

One possible payload a work rover could expect is lunar regolith. The LROP was sized to a hypothetical regolith transport vehicle. To obtain the desired volume of regolith, the payload mass was divided by the recommended specific gravity of lunar soils, 3.1g/cm^3 (Carrier 2005). This .0225 m^3 volume was then scaled up by an order of magnitude to be able to accommodate a wide range of soil densities. This volume drove the dimensions of the platform. The length, width, and height of the LROP were

based on the some of the mobility characteristics such as turn radius, CG height, and skid steer stresses. In order to obtain adequate turn radii and minimize the stresses induced by a skid steer point turn a wheel track to base ratio of at least 1.3 was selected. The last dimensional bound was a ground clearance of 25 cm while having a stable CG height based on FEM tipping analyses that were conducted. When all these bounds were considered a rover frame of 91.4 x 55.88 x 41.9 cm was selected to represent the payload volume of equivalent regolith.

The payload volume is represented by the rectangular aluminum frame and the vertical weight bar's height in figure 1. The frame is comprised laterally of aluminum rail stock bar and longitudinally of aluminum square channel. The weights sit on another aluminum rail stock bar. These rails allow for the varying of the CG both in the lateral and longitudinal direction. The frame and CG system was constructed out of aluminum for its strength and ease of incorporating rails. The CG variability feature was included after seeing Wettergreen's (2010) Scarab rover actively control its CG, allowing it to ascend steeper slopes by redistributing load across its wheels. Studying the sensitivity of varying the CG was one of the things this platform was designed to do.

Figure 1: Lunar Rover Optimization Platform (LROP).

The CG is controlled by adding payload to the vertical weight rod and then sliding its bracket forward, aft, or laterally (Fig. 2). This feature could help understand the impact of design changes such as the relocation of a rover's navigation mast as was the case with the FIDO rover. The FIDO rover was a development rover for the MER used to prove out the navigation systems (Tunstel 2002). The main difference to the flight rover was its mast being located in the rear of the vehicle versus the front. This represented a change in CG which was important for mobility system designers to characterize. The CG rail system on the LROP is part of the frame. The load from the payload is transferred through the frame to the main axel and a vertical suspension rod.

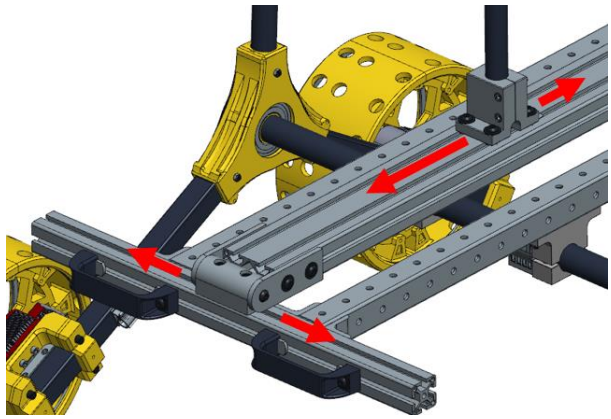

Figure 2: CG adjustment rail system.

The main axel is made out of axially optimized carbon fiber and supports the frame with two saddle clamps (Fig.2). The vertical suspension rod connects to the frame with saddle clamps as well and is made of aluminum. The vertical rod supports a bearing upon which the suspension system pivots about (see appendix).

2.2 Wheel choice

Mass optimization also informed the wheel count selection. A four wheeled configuration with an averaging arm was evaluated against a six wheeled rocker-bogie with differential. Although the rocker bogie suspension has been proven to allow for traversal of obstacles up to 1.5 times the wheel diameter it is has a higher part count (Hayati 1997). This success in obstacle traversal was especially important during missions like the Mars Pathfinder (MPF) Sojourner rover, because of the rover's size. The MPF was in the micro class and had wheels that were 6.5 cm in radius. In its mission it was possible that it could encounter 18 cm obstacles so the rocker bogie was selected as a suspension system. The issue is not as pronounced with medium class rovers since the scaling of the wheels means that same 18 cm obstacle is now being traversed by an 12.06 cm radius wheel as is the case with LROP. Sutoh (2010) suggests that wheel diameter is more impactful than wheel width in reducing wheel sinkage. The LROP's wheels being 24.13 cm in diameter and 11.43 cm wide would be sufficiently large to traverse an 18 cm obstacle without excessive sinking (Miller 2007).

Ultimately a four wheel design was selected because it would require less motors, wheels, and cabling driving the weight down. For the prove-out tests of the LROP, a rigid wheel was designed. A rigid wheel was selected to be able to assume that the effective radius is equal to the actual radius under nominal conditions simplifying analysis. The wheel does not have any crowning, again, to simplify ground contact analysis. This design did not have any grousers/lugs to isolate the friction mechanics during obstacle traversal. The lightening holes on the wheel were introduced to lower their weight. These holes are eventually covered by the 100 grit abrasive tape added to the circumference of the wheel. The tape was added to interact with the 100

grit abrasive tape of the test track to achieve a zero slip condition on the wheel when the rover is cruising over level ground.

The wheel was segmented into four pieces to adopt a modular design which could be printed in-situ on lunar bases. It was also driven by the build volume of the 3d printers being used for this project. The wheel segments were connected with ribs on the wheel's inner lip (Fig.3). These ribs spanned the joints creating a circular load path for the wheel. The four segments then attach to a hub that connects to the platform's motors. This construction could be made possible with ferrosilicon alloy materials that are extracted from lunar soil. These materials can potentially be used in wire based additive manufacturing on the moon (Grossman 2019). The additive manufacture of rover wheels has been explored by the Hakuto rover's designers. They will use wheels printed out of Ultem on their flight rover in 2019 (Walker 2017). Once their design is flight proven on the moon there will be a push to see if a version of the wheel could be printed out of a ferrosilicon alloy to prove out the possibility of a sustainable rover fleet on the moon. The LROP will aid this push by proving another conceptual design for such a wheel architecture.

Figure 3: LROP's segmented wheel design.

2.3 Rapid Prototyped Parts

Much like the wheels other components of the LROP were additively manufactured to continue with the architecture of future parts possibly printed on the moon. Although the parts were made of PLA their design took into account directional strengths of the orthotropic material generated by the fused deposition printing process. The rapid prototyping also lowered the cost and improved the manufacturing time.

2.4 Suspension

The four wheeled configuration was paired with a passive suspension system and averaging arm. This suspension system coupled the left and right sides of the rover. The coupling worked as follows: if the front left wheel encountered an obstacle and pitched up, the rear left would pitch down and remain in contact with the ground. All the while the rear right would pitch up as well and the front right would pitch down (Fig. 4). This architecture allowed the rover to passively distribute its wheel loading

while traversing obstacles or ascending slopes. Despite it having some load leveling, a lack of sufficient load distribution is what resulted in the unfortunate embankment of the Opportunity rover on Mars, (Arvidson 2011). This suspension design also allowed the torque generated by loads off the CG to be countered by the vertical rods of the suspension system instead of gear teeth as would be the case in a rocker bogie with a differential. This feature expanded the payload capacity of the LROP while minimizing weight.

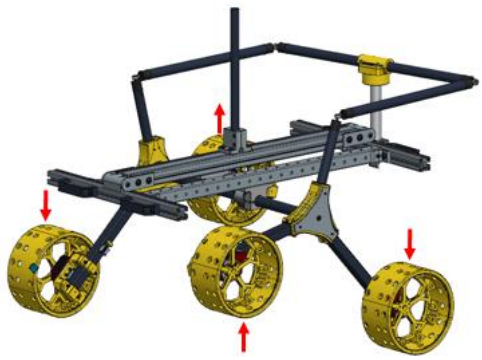

Figure 4: LROP's passive suspension.

2.5 Tether

The LROP has a motor on every wheel, this reduced the need for a drive train and enables skid steering. HEBI X8-16 actuators were selected for propulsion. These actuators have the ability to feed back: XYZ position, velocity, torque, accelerations, current, voltage, and temperature amongst other things. This suite of data in one compact package made them desirable for weight reduction. To further reduce the weight of the vehicle, data and power were delivered to the motors via a tether that trailed behind the rover. During testing the tether is held up to prevent the drag corrupting the torque data.

2.6 Design Overview

Table 1: Design Parameters

Parameter	**Value**	
Platform LxWxH:	104 cm x 102 cm x 82.6 cm	(41 in x 40.2 in x32.5 in)
Platform dry mass:	20.4 kg	(45 lb)
Payload LxWxH:	91.4 cm x 55.9 cm x 41.9cm	(36 in x 22 in x 16.5 in)
Payload capacity	70 kg	(155 lb)
Wheel base:	65.6 cm	(25.8 in)
Wheel track:	91.1 cm	(35.8 in)
Base/Track Ratio:	1.389	
Ground Clearance:	27.1cm	(10.6 in)
Wheel diameter:	24.13 cm	(9.5 in)
Max wheel diameter:	63.5 cm	(25 in)
Wheel width:	11.43 cm	(4.5 in)
Wheel loading:	5 – 22.5 kg	(11 – 50 lb)

3. LROP Testing

In order to validate the wheel and vehicle testing capabilities of the LROP two styles of experiments were conducted: obstacle traversal and slope ascent. During these prove out tests the CG and mass fraction (MF) of the LROP were varied.

3.1 Obstacle traversal

The two variables that were targeted for these tests were obstacle height and obstacle angle of attack (AOA) vs CG position. The obstacle selected was a piece of slate that was wider than the LROP. The slate was raised to a desired height (7.6 cm) and leveled to a constant elevation, otherwise known as a step obstacle (Fig. 5). The AOA was determined by marking angles on the starting platform every 5° from 0°-20°, with 0° being a head-on approach to the obstacle.

Figure 5: Step obstacle.

The LROP was lined up by mounting a laser line level (Fig. 6). The CG was varied by shifting the weight rack and using vehicle scales and the method described by Mango (2014). For this round of testing the CG was only varied longitudinally forward and aft 10% and a mass fraction of 1.55 (31 kg payload) was selected. The CG was only varied 10% for these initial tests to prevent the tipping of the rover during testing at large slope angles. A +10% CG shift meant the weight was shifted forward and conversely for -10%.

The test were judged on a pass, half pass, and fail basis. A full pass meant the LROP got all four wheels over the step obstacle. A half pass meant that LROP only had the forward wheels traverse the obstacles and a failure was when no wheels were able to traverse. The results of these tests are outlined in table 2.

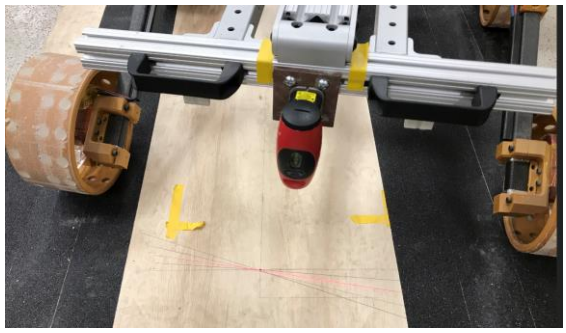

Figure 6: Angle of attack alignment.

Table 2: Angle of attack vs. center of gravity location for a 7.6 cm high step obstacle.

Obstacle Traversal					
	Angle of Attack				
CG Location	0°	5°	10°	15°	20°
-10%	Half Pass	Half Pass	Full Pass	Full Pass	Full Pass
Centered	Full Pass	Full Pass	Full Pass	Full Pass	Full Pass
+10%	Fail	Fail	Full Pass	Full Pass	Full Pass

3.2 Slope Ascent

For these tests the LROP was put into Glenn Research Centers Simulated Lunar Operations (SLOPE) adjustable tilt bed. The tilt bed holds GRC-1 lunar simulate which was prepared to "loose" soil conditions to represent the similar terrain strength and deformation properties found on the moon (Oravec 2010). The loose soil condition is the most challenging condition for mobility platforms since the wheels have a higher level of sink and slip in it, this which why it was selected. The tilt bed was adjusted to 0°, 10° and 20°. The LROP was to undertake a head-on path to gage the effect of CG change on ascent. Success was also measured on a pass, half pass, and fail basis for these tests. A pass was given when the LROP ascended with very minimal sinkage and slippage. A half pass was awarded when the LROP had moderate sinkage or slippage but still made at least one wheel diameter's worth of forward progress under steady state. A fail was given when the LROP did not make notable forward progress due to the wheels slipping. For these tests the mass fraction of .55 was selected (11.3 kg payload) and the CG was evaluated at 10% forward and aft longitudinally. The results of these tests are outlined in table 3.

Table 3: Slope ascent vs. center of gravity location.

Slope Ascent			
	Slope Angle		
CG Location	0°	10°	20°
-10	Full Pass	Half Pass	Fail
Centered	Full Pass	Half Pass	Fail
+10	Full Pass	Full Pass	Fail

4. Conclusion

After prove-out testing it was concluded that a testing platform was created that could produce meaningful traction data for different wheel designs and CG changes. Testing showed that the larger the AOA to an obstacle the more successful traversal will be. The testing also showed that a forward shift in CG aids in the traversal of a slope. This is most likely due to the even distribution of load on all the wheels of the rover. These results hold true for the LROP in its current configuration. The LROP is a tool that can help future rover designers quickly explore the options and sensitivities for their medium class rovers. This is especial true when the LROP is coupled with the capabilities of GRC's SLOPE lab. In the future the research team will explore the effects of AOA of obstacle traversal has on power consumption for various wheel designs including meshed spring tires. This benefits the rover design community as well as the ISRU community which can count on the integration of reliable mobility platforms into the sustainable off-world future that NASA envisions.

5. Acknowledgements

The authors would like to express their appreciation to Erin Rezich and Thomas Fransua for their help in the testing. To Richard Manco for his help in manufacturing and assembly. Finally, to Collin Creager for technical direction and professional input.

6. References

Hayati, S., Volpe, R., Backes, P., Balaram, J., Welch, R., Ivlev, R., Tharp, G., Peters, S., Ohm, T., Petras, R., and Laubach, S. (1997). "The Rocky 7 rover: a Mars sciencecraft prototype." *Proceedings of International Conference on Robotics and Automation*.

Sutoh, M., Yusa, J., Nagatani, K., and Yoshida, K. (2012). "Traveling performance evaluation of planetary rovers on loose soil." *Journal of Field Robotics*, 29(4), 648–662.

Miller, D., Ravine, M. (2007). "Semi-autonomous Rover Operations: An Integrated Hardware and Software Approach for More Capable Mars Rover Missions."

Grossman, K. D., Sakthivel, T. S., Sibille, L., Mantovani, J. G., and Seal, S. (2019). "Regolith-derived ferrosilicon as a potential feedstock material for wire-based additive manufacturing." *Advances in Space Research*, 63(7), 2212–2219.

Costes, N., Farmer, J., George, E. (1972). "Mobility Performance of the Lunar Roving Vehicle: Terrestrial Studies – Apollo 15 Results." *NASA TR*, R-401

Mango, N. (2004). "Measurement & amp; Calculation of Vehicle Center of Gravity Using Portable Wheel Scales." *SAE Technical Paper Series*.

Carrier, D., Olhoeft, G., and Mendell, W. (1991). "Physical Properties of The Lunar Surface." *Lunar Sourcebook: A User's Guide to the Moon*, Cambridge University Press, 475–483.

Tunstel, E., Huntsberger, T., Aghazarian, H., Backes, P., Baumgartner, E., Cheng, Y., Garrett, M., Kennedy, B., Leger, C., Magnone, L., Norris, J., Powell, M., Trebi-Ollennu, A., and Schenker, P. (2002). "FIDO rover field trials as rehearsal for the NASA 2003 Mars Exploration Rovers mission." *Proceedings of the 5th Biannual World Automation Congress*.

Oravec, H., Asnani, V., Zeng, X. (2010). "Design and Characterization of GRC-1: A soil for lunar terramechanics testing in Earth-ambient conditions." *Journal of Terramechanics*, 47(6), 361-377

Arvidson, R.E., Ashley, J.W., Bell III, J.F., Chojnacki, M., Cohen, J., Economou, T.E., et al. (2011). "Opportunity Mars Rover Mission: Overview and Selected Results from Purgatory Ripple to Traverses to Endeavour Crater." *Journal of Geophysical Research*, 116

Wettergreen, D., Moreland, S., Skonieczny, K., Jonak, D., Kohanbash, D., and Teza, J. (2010). "Design and field experimentation of a prototype Lunar prospector." *The International Journal of Robotics Research*, 29(12), 1550–1564.

Walker, J. (2017) "Final configuration of the ispace Hakuto Rover for a Google Lunar XPRIZE mission." *International Astronautically Congress*.

7. Appendix

Rover nomenclature: